Current Biology *18*, 566–575, April 22, 2008 ©2008 Elsevier Ltd All rights reserved DOI 10.1016/j.cub.2008.03.049

Article

Ino80 Chromatin Remodeling Complex Promotes Recovery of Stalled Replication Forks

Kenji Shimada,[1,6] Yukako Oma,[2,6] Thomas Schleker,[1,5] Kazuto Kugou,[3,4] Kunihiro Ohta,[3,4] Masahiko Harata,[2,*] and Susan M. Gasser[1,*]

[1]Friedrich Miescher Institute for Biomedical Research
Maulbeerstrasse 66
CH-4058 Basel
Switzerland

[2]Laboratory of Molecular Biology
Graduate School of Agricultural Science
Tohoku University
Tsutsumidori-Amamiyamachi 1-1
Aoba-ku, Sendai 981-8555
Japan

[3]Shibata Distinguished Senior Laboratory
RIKEN Discovery Research Institute
Hirosawa 2-1
Wako, Saitama 351-0198
Japan

[4]Department of Life Sciences
Graduate School of Arts and Sciences
The University of Tokyo
Komaba 3-8-1
Meguro-ku, Tokyo 153-8902
Japan

Summary

Background: Chromatin remodeling complexes facilitate the access of enzymes that mediate transcription, replication or repair of DNA by modulating nucleosome position and/or composition. Ino80 is the DNA-dependent Snf2-like ATPase subunit of a complex whose nucleosome remodeling activity requires actin-related proteins, Arp4, Arp5 and Arp8, as well as two RuvB-like DNA helicase subunits. Budding yeast mutants deficient for Ino80 function are not only hypersensitive to reagents that induce DNA double-strand breaks, but also to those that impair replication fork progression.

Results: To understand why *ino80* mutants are sensitive to agents that perturb DNA replication, we used chromatin immunoprecipitation to map the binding sites of the INO80 chromatin-remodeling complex on four budding yeast chromosomes. We found that Ino80 and Arp5 binding sites coincide with origins of DNA replication and tRNA genes. In addition, Ino80 was bound at 67% of the promoters of genes that are sensitive to *ino80* mutation. When replication forks were arrested near origins in the presence of hydroxyurea (HU), the amount of INO80 complex at stalled forks and at unfired origins increased selectively. Importantly, the resumption of DNA replication after release from a HU block was impaired in *ino80* mutants. These cells accumulated double-strand breaks as they attempted to restart replication. Consistently, *ino80*-deficient cells, although proficient for checkpoint activation, delay recovery from the checkpoint response.

Conclusions: The INO80 chromatin remodeling complex is enriched at stalled replication forks, where it promotes the resumption of replication upon recovery from fork arrest.

Introduction

Eukaryotic genomes are packaged into nucleosomes, which generally reduce accessibility for enzymes that mediate DNA-based cellular processes such as transcription, replication, or the repair of DNA damage. To help overcome this nucleosomal barrier, all eukaryotic cells possess several classes of ATP-dependent chromatin-remodeling complexes. These function by repositioning and removing nucleosomes or by exchanging histone variants to alter chromatin conformation [1]. The role of the four major classes of nucleosome remodelers in transcription is well documented. Yet, in some cases, several of the strains deficient in nucleosomal remodelers show a hypersensitivity to DNA-damaging agents that cannot be explained by their transcription-modulating activities. Indeed, recent studies implicate INO80-, SWR1-, and RSC-remodeling complexes directly in DNA repair, most notably at double-strand breaks (DSB) or sites of γ-irradiation-induced damage [2–10].

The Ino80 chromatin remodeler is of particular interest in this respect. Ino80 is part of a large complex (INO80 complex) containing 15 subunits in *S. cerevisiae* [5, 11] and 13 in human cells [12]. Among these are the conserved actin-related proteins Arp4 (BAF53), Arp5, and Arp8, as well as Rvb1/Rvb2 (TIP49a/TIP49b in mammals), a RuvB-related DNA helicase. Budding yeast harbors a second, closely related DNA-dependent ATPase called Swr1 that also forms a multisubunit complex containing Rvb1/Rvb2 and Arp4. This complex resembles SRCAP in mammals and both function by exchanging H2A for the histone H2A.Z variant [2–4]. SRCAP also shares subunits with the mammalian Tip60 complex, which provides histone acetyltransferase activity to modify histone H3 and H4 N-terminal tails in nucleosomes surrounding DSBs (reviewed in [13]).

In budding yeast both INO80 and SWR1 complexes are recruited to DSBs in response to H2A phosphorylation (γH2A) by the ATM-related Tel1 and Mec1 enzymes, although only the INO80 complex serves to remove γH2A and core histones near the break [7, 8]. Mutations in the INO80-specific subunits Arp8 or Nhp10 impair the binding of Mre11 nuclease, yKu80, and the Mec1-Ddc2 kinase at DSBs, resulting in defective end-resection and checkpoint activation (reviewed in [14]). Mutants lacking Swr1 do not have equivalent defects [8]; thus, in yeast the complex containing Ino80, but not Swr1, appears to contribute to processing of breaks for DSB repair.

In mammals the INO80 complex also has been implicated in promoting repair by homologous recombination [10]. The human INO80 complex contains the Polycomb-group protein YY1, which is not conserved in budding yeast. Reduced levels of YY1 or Ino80-rendered cells hypersensitive to DNA-damaging agents and deficient for homology-directed repair of chromosomal DSBs [10]. It is proposed that YY1, which binds the

*Correspondence: mharata@biochem.tohoku.ac.jp (M.H.), susan.gasser@fmi.ch (S.M.G.)

[5]Present address: European Institute of Oncology, IFOM-IEO-CAMPUS, Via Adamello 16, I-20139 Milano, Italy.

[6]These authors contributed equally to this work.

Rvb1/2 subunits TIP49a and TIP49b, recruits the complex to damage by directly recognizing recombination structures.

It remained unexplained why *ino80* mutants in budding yeast are hypersensitive to arrest by hydroxyurea (HU) [6], which stalls forks, but unlike MMS does not necessarily generate DNA breaks. Indeed, in budding yeast sensitivity to HU often reflects an inability of replication polymerases to remain engaged at stalled forks and restart synthesis after a prolonged arrest (reviewed in [15]). To examine the role of INO80 complex in replication events, we have mapped Ino80 and Arp5 binding under both unperturbed and fork-stalling conditions. We find that both components of the complex are frequently present at yeast origins of replication (ARS elements) even in the absence of damage. INO80 complex is recruited at even higher levels to replication forks when they stall on HU. Cells deficient for Ino80 remodeling activity show defects in replication fork restart, generating DSBs, and delaying recovery from the intra-S-phase checkpoint arrest.

Results

INO80 Complex Is Found at Origins of Replication and at tRNA Genes

To understand the function of the INO80 complex, we have mapped its binding sites over four *S. cerevisiae* chromosomes by hybridizing DNA recovered from chromatin immunoprecipitation (ChIP) to tiled microarrays of chromosomes 3, 4, 5, and 6R (ChIP-chip) [16]. Antibodies specific either for Arp5 or for Myc-tagged, endogenously expressed Ino80 itself were used on lysates prepared from cells that were formaldehyde-fixed during exponential growth.

The chromosome-wide distributions of Ino80 and Arp5 are nearly identical (Figure 1A and Figures S1–S3 available online). Indeed, Arp5 is an integral component of the INO80 complex, essential for its nucleosome remodeling activity in vitro [17]. INO80 complex binding sites map primarily to intergenic regions, yet their distribution was clustered. We detected contiguous zones ranging in size from 40 to 120 kb that were either consistently enriched or consistently depleted for the INO80 complex (Figures S1–S3). The underlying cause of this distribution is unknown; we find no significant correlation with gene density or the previously described AT- or GC-isochores that characterize yeast chromosomes [18–20].

Consistent with its role in gene regulation, INO80 complexes were mapped to many promoters. Among those genes known to be regulated by Ino80 under unperturbed growth conditions [6], roughly two-thirds showed enrichment for Ino80 (67%) and Arp5 (60%) within 1 kb of the transcriptional start site (data not shown). Nonetheless, this value is relatively low when compared to equivalent measurements made for Swr1 and its subunit Arp6, which were found at 87% of the promoters that require it for efficient repression (T. Yoshida and M.H., unpublished data). More surprising was the correlation of Ino80 and Arp5 signals with sites of initiation of DNA replication (autonomously replicating sequences or ARS, indicated by red arrows in Figure 1A and Figures S1–S3). Not all ARS elements were Ino80 positive in exponentially growing cells, yet Ino80 binding was detected more frequently at origins than could be expected by randomized interaction based on hypergeometrical distribution calculations ($p = 0.020$). To understand whether a specific subset of origins selectively bind the INO80 complex, we classified the origins by their timing of initiation. As shown in Table 1, INO80 complex binding in unperturbed cells was found most frequently, but not exclusively, at origins that fire early in S phase. Nonetheless, the degree of enrichment at origins was lower for Ino80-myc than for Orc1 or Cdc45 [16]. This could stem either from cell-cycle variations in Ino80 binding or low-crosslinking efficiency.

A second class of chromosomal loci strongly associated with Ino80 was that of tRNA genes (Figure 1A, black arrows). Of the 114 tRNA loci scored, 93% were positive for Ino80 in exponentially growing cells, as well as in synchronized G1- and S-phase cells (Table 1, Figures S1–S3, and data not shown). The tRNA genes are known to be natural pause sites for replication forks [21], and progression through tRNA requires Rrm3, a DNA helicase that progresses with the replication machinery [22]. Interestingly, yeast strains lacking the INO80 complex subunit *arp8* show similar profiles of synthetic growth defects as the *rrm3* null mutant (bioPIXIE database [23]). The defects are not additive when combined in a double mutant, however, suggesting that the INO80 complex and Rrm3 may function on a common pathway.

INO80 Complex at Origins Increases upon HU-Induced Arrest of Replication Forks

Given the presence of Ino80 at origins and tRNA genes, we examined whether its presence might reflect a function for the remodeler at sites where DNA polymerases are paused. If Ino80 was selectively recruited to damage, one might expect this binding to be S phase specific. To examine this we performed ChIP-chip analysis for Ino80 precipitated from cells arrested in G1 by treatment with pheromone (α-factor) and after their synchronous release into 0.2 M HU. Under these conditions replication forks stall within 5 kb of early origin initiation zones [16]. In G1-phase cells the distribution of Ino80 was nearly identical to that observed for a random population: some, but not all, origins were positive. In cells treated with HU, we note a significant increase in both frequency and abundance of Ino80 at origins of replication (Table 1). Even origins that had levels of Ino80 below our threshold of detection in G1-phase cells became positive when the culture was treated with HU (Figure 1B).

One might imagine that the INO80 complex binds to all sites in an enhanced manner in S-phase cells. To see if the increase we scored at origins on HU was specific to forks that arrest within a few kb of early firing origins, we plotted the ChIP-chip values for all loci in G1-phase cells (α-factor arrest; x axis) versus the values obtained in HU-arrested cells (y axis). The mean increase of Ino80 at ARS elements was significantly more than at other loci (Figure 1C, compare regression lines for all ARS elements versus all loci). The binding of Ino80 at tRNA genes did not increase in a similar manner (Figure S4), consistent with the fact that tRNA genes do not generally flank origins. Intriguingly, there were seven origins at which Ino80 binding did not increase on HU, and almost all of these fall in repressive chromatin environments. Two are inactive origins at silent mating type loci (ARS301 and ARS317), and four are late firing (ARS410, ARS443, ARS522; and ARS319 in the subtelomeric core X element), suggesting that silent chromatin may be refractory to the INO80 complex.

INO80 Binding Correlates with DNA Polymerase Arrest at Early-Firing Origins

To determine whether the increase in Ino80 binding on HU parallels the stalling of replication polymerases, we monitored both DNA polymerase ε and Ino80 by ChIP at an early-firing origin after their dynamics as cells synchronously enter S phase and arrest replication due to nucleotide depletion. We maximized the efficiency of Ino80 recovery by exploiting a novel biotin

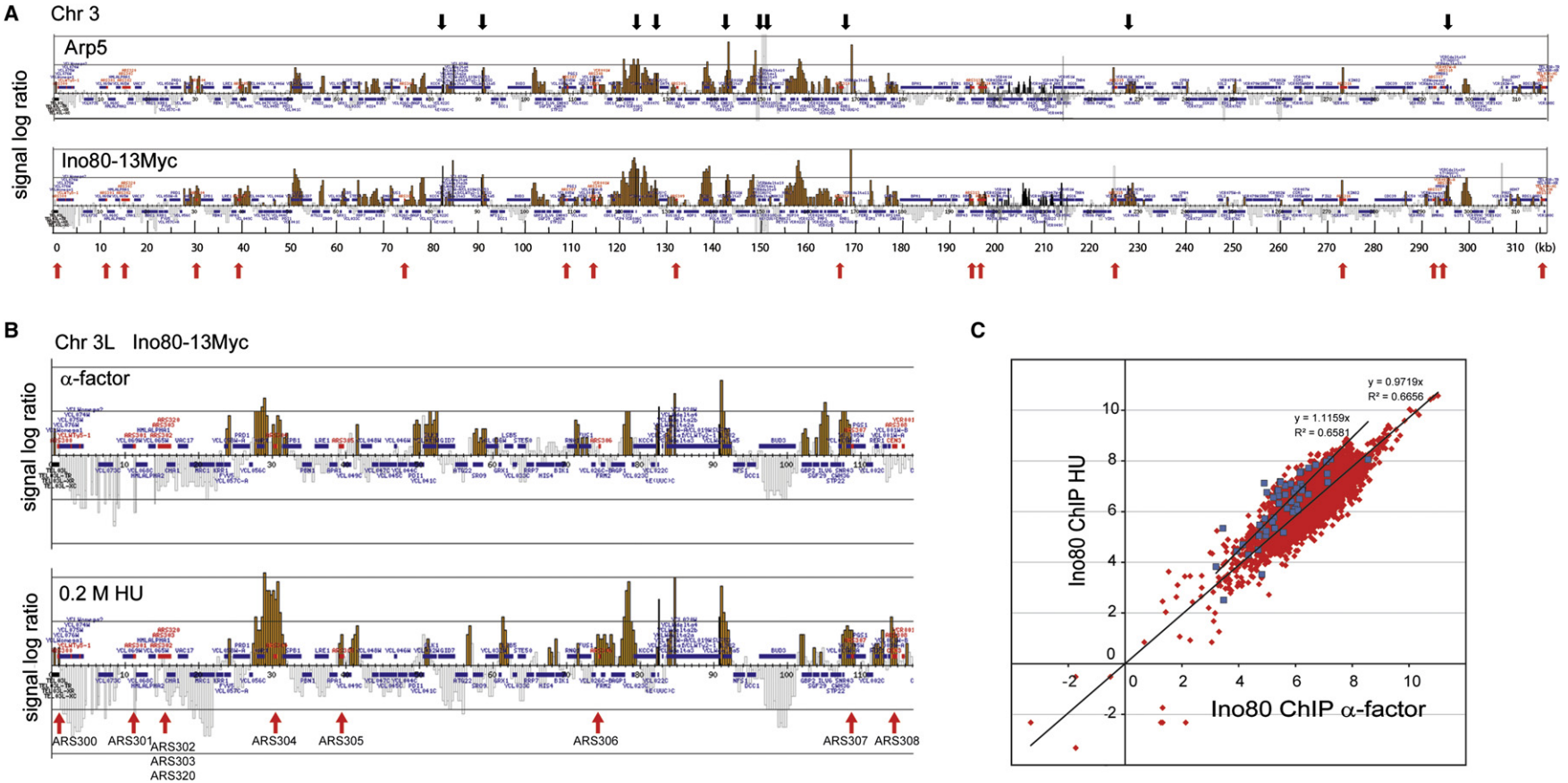

Figure 1. Localization of the INO80 Complex on Yeast Chromosomes

(A) ChIP-chip analysis was performed with anti-Arp5 (top) or anti-Myc antibody (bottom) on lysates from cell bearing Ino80-13myc as the only tagged locus. Random cultures of cells were crosslinked with formaldehyde and lysed for ChIP as described in the Experimental Procedures. Data from yeast Chr 3 are shown and data from other chromosomes (Chr4, Chr5, and Chr6R) are shown graphically in Figures S1–S3. Vertical bars represent the binding ratio of proteins in each locus. The loci, which cover 300 bp and 150 bp regions, are shown by yellow and black vertical bars, respectively. The scale of the vertical axis is the signal log ratio [49], and the horizontal axis shows kilobase units. Red arrows indicate the position of replication origins (ARS), and black arrows indicate tRNA genes.

(B) ChIP-chip analysis was performed with anti-Myc mAb on lysates from cells bearing Ino80-13myc as the only tagged locus. Cells were arrested in G1 with α-factor for the first sample (top) and then synchronously released in 0.2 M HU for 60 min as the second sample (bottom). Data from the left arm of yeast Chr3 are shown. Arrows indicate the positions of replication origins (ARS).

(C) ChIP-chip analysis for Ino80-13myc was performed in cells arrested in α-factor or in HU. The enrichment of Ino80-13myc in HU (vertical axis) is plotted against the enrichment on α-factor (horizontal axis) as red diamonds. The blue squares indicate Ino80-13myc signals at ARS. The scale of the axes is the $\log_2$ value of the hybridization signals [49]. The regression lines for all loci (lower line) and for all ARS loci (upper line) are shown.

Table 1. Summary of Ino80 Presence at Replication Origins and tRNA Genes

Replication Origins

Origin Timing[a]	Number of Origins Counted	Origins Ino80-Positive in G1[b]	% Positive in G1[c]	Origins Ino80-Positive in HU[b]	% Positive in HU
early	36	17	47	32	89
middle	56	17	30	49	88
late	26	7	27	21	81
total	118	41	35	102	86

tRNA Genes[d]

	Number of tRNA Genes	Number of tRNA Loci Counted[e]	Ino80-Positive tRNA Loci[e,f]	% of tRNA Loci Positive[g]
Chr3	10	14	10	71
Chr4	28	50	47	94
Chr5	20	36	36	100
Chr6R	8	14	13	93
total	66	114	106	93

[a] Classified as early (replication index: RI < 0.2), middle (0.2 ≤ RI < 0.45) or late replicating (RI ≥ 0.45) based on OriDB (DNA replication origin database [50]).
[b] Scored from two experiments for G1 cells blocked with α-factor and in cells synchronously released into 0.2 M HU.
[c] We note that G1 phase results parallel those detected in a nonsynchronized culture (data not shown).
[d] In exponential growing cells.
[e] Pooled data from two independent experiments.
[f] Scored as described in Figure 1.
[g] We note that this level does not increase significantly on HU (Figure S4).

tagging system [24] that allows stringent washing prior to analysis by quantitative PCR. Yeast cells were reversibly arrested with α-factor and released into 0.2 M HU for 20, 40, and 60 min. Both DNA pol ε and Ino80 levels increased rapidly at ARS607 and at +4 kb from the initiation zone as replication forks accumulated in this zone for up to an hour (Figure 2A). This ChIP

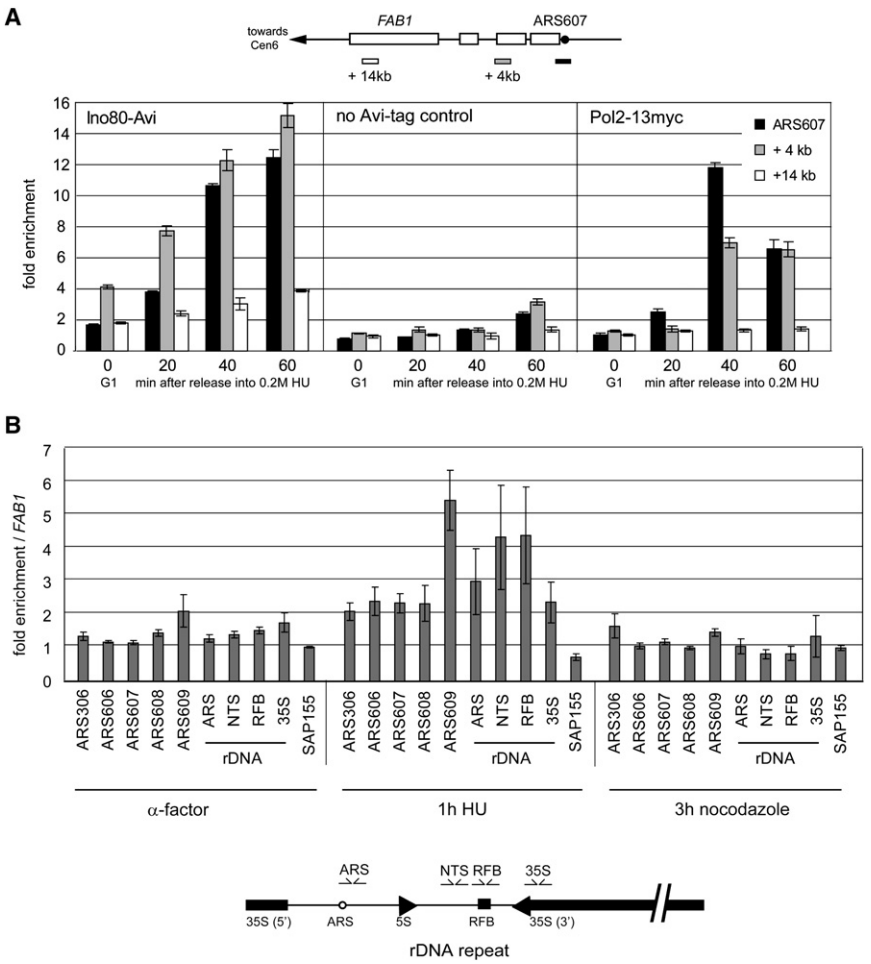

Figure 2. The Increase in Ino80 near Origins on HU Parallels the Binding of Stalled Replication Polymerases

(A) Cells bearing a genomic copy of Ino80-Avi tag and an isogenic nontagged strain, both carrying pRS415-NLS-BirA, were cultured with biotin to allow tagging of Ino80. These cells and cells bearing Pol2-13myc [48] were synchronized in G1 with α-factor and then released into 0.2 M HU. ChIP samples were taken after 0, 20, 40, and 60 min in 0.2 M HU and analyzed by real-time qPCR for ARS607 and for loci +4 kb and +14 kb from ARS607 [48]. We note that Ino80 levels in G1 are slightly higher at +4kb than at the origin, probably reflecting its binding to the promoter of the gene *ATG18* found at this site (see map). The fold enrichment is plotted over a background control of TK gene (see the Experimental Procedures). Error bars represent the standard error of four PCR reactions.

(B) Ino80 association at ARS elements and at the rDNA replication fork barrier increases in HU-blocked cells. Cells bearing a genomic copy of Ino80-13myc were cultured in α-factor (left panel) or were subsequently released into YPD medium containing 0.2 M HU for 60 min (middle). For G2/M-phase arrest, cells were cultured in 15 μg/ml nocodazole for 3 hr (right panel). ChIP samples obtained with Ino80-13myc were analyzed by qPCR for sequences at the following ARS elements (306, 606, 607, 608, and 609), at rDNA loci (rDNA ARS; NTS, nontranscribed region; RFB, replication fork barrier; and 35S, 35S rRNA gene), and at control loci (*FAB1* and *SAP155*). In this panel, Ino80-13myc signal intensity is plotted as a fold enrichment over the signal at *FAB1* (+14 kb from ARS607), which showed little or no variation on HU (see [A]). Error bars represent the standard error of three independent experiments.

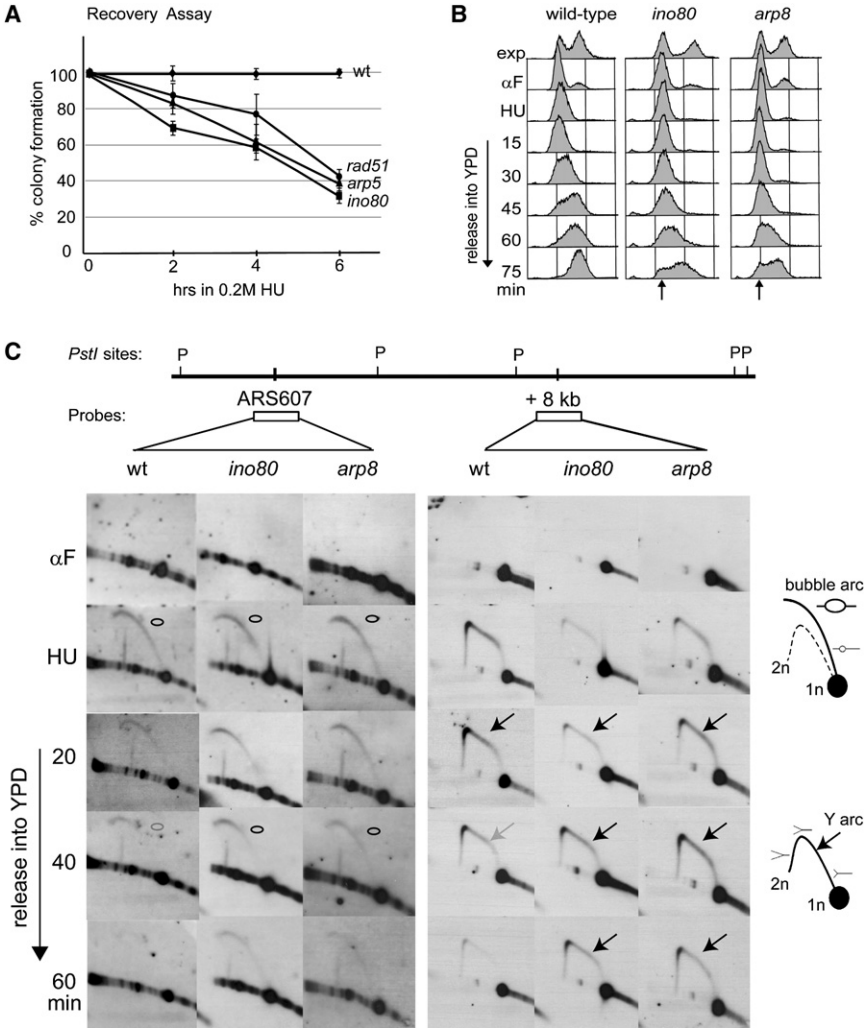

Figure 3. *ino80* and *arp8* Mutations Impair Resumption of Replication after HU Treatment

(A) A wild-type strain (GA-2263) and isogenic disruptions for either *ino80*, *arp5*, or *rad51* were arrested in α-factor then released into 0.2 M HU and held for 0, 2, 4, and 6 hr. Cells were then plated in triplicate onto rich media without HU (YPD) and colony formation was scored after 3 days at 30°C. Wild-type strain values are used for normalization (100%). Error bars represent the standard deviation of triplicates.

(B) Wild-type, *ino80*, and *arp8* cells were synchronously released into 0.2 M HU as in (A) for 90 min. Cells were then washed and released into fresh YPD, and samples were taken for FACS analysis. We could monitor a delay in progression from G1 into S phase in the absence of *ino80* when an unperturbed cell cycle was monitored by FACS (data not shown). This is likely to reflect Ino80-dependent changes in G1 transcriptional events [4, 6] because early-origin firing is unaffected by the mutation (C).

(C) Two-dimensional gel analysis was performed on the cell samples taken for FACS in (B) at the indicated time points. PstI digested genomic DNA was analyzed by 2D gels probed for ARS607 and a site at +8 kb from ARS607.

data suggests that INO80 associates not only with origin-bound complexes but also with stalled replication forks.

We tested the generality of this observation by quantifying Ino80 ChIP signal at several other origins in cells arrested either in G1, in S phase with HU, or in G2/M with nocodazole (Figure 2B). The amount of Ino80 recovered at replication origins in HU-arrested cells increased reproducibly by 2- to 3-fold (Figure 2B), whereas in nocodazole, the values generally dropped. In nocodazole the values generally were lower than on HU. Ino80 ChIP at the gene *SAP155* served as a control for origin specificity; its low level of Ino80 binding at this locus did not fluctuate under the conditions tested.

We also monitored the presence of Ino80 within the rDNA array because each rDNA repeat unit contains a replication fork barrier (RFB) that blocks replicative polymerases in a unidirectional manner [25, 26]. Consistent with the observed accumulation of Ino80 and DNA pol ε near ARS607 in HU-treated cells, we see a selective enrichment of Ino80 protein at the replication fork barrier in the rDNA (Figure 2B).

Intriguingly, the accumulation of INO80 complex at origins on HU is not restricted to those that initiate replication early (Table 1 and Figure 2B). We also scored an increase in Ino80 signal at late-firing origins during the arrest in HU even though the checkpoint kinase Rad53 represses the initiation of replication at these origins on HU [27]. With respect to late origins, our data argue that enhanced Ino80 recruitment occurs before replication initiation.

ino80 Mutants Delay Recovery from Replication Fork Stalling

Finding the INO80 complex accumulating at stalled replication forks prompted us to test whether its remodeling function is necessary for the resumption of DNA replication. This can be quantified by scoring the ability of cells to form colonies after prolonged exposure to 0.2 M HU. Wild-type cells show a robust ability to recover, with less than a 10% drop in viability after a 6 hr treatment in HU [28]. Deletion of either *ino80* or *arp5*, on the other hand, reduced colony forming units by 60% (Figure 3A). This is similar to the drop in viability observed with mutants in the recombination-mediating component Rad51 but is less severe than that scored for cells lacking the ATR kinase Mec1 [28, 29].

To see if the drop in viability reflects impaired replication fork resumption after HU arrest, we monitored DNA synthesis by FACS and 2D gel analysis during recovery from arrest on HU. First, we note that in the absence of HU, wild-type and mutant cells progress through S phase with roughly equal kinetics, although origin firing is somewhat less synchronous in *ino80* mutants (Figure S5). When wild-type, *ino80*, and *arp8* cells were synchronously arrested in 0.2 M HU for 1.5 hr and then allowed to resume growth in fresh medium, FACS analysis shows delayed S-phase progression in *ino80* and *arp8* cells (Figure 3B). Indeed, wild-type cells typically completed replication by 75 min, yet unduplicated genomes persisted beyond 75 min in the mutant (Figure 3B).

Analysis of replication intermediates by 2D gel electrophoresis confirmed that loss of Ino80 function delays the completion of DNA replication after fork arrest. Two-dimensional gels were probed for the early-firing origin ARS607 to monitor the "bubble

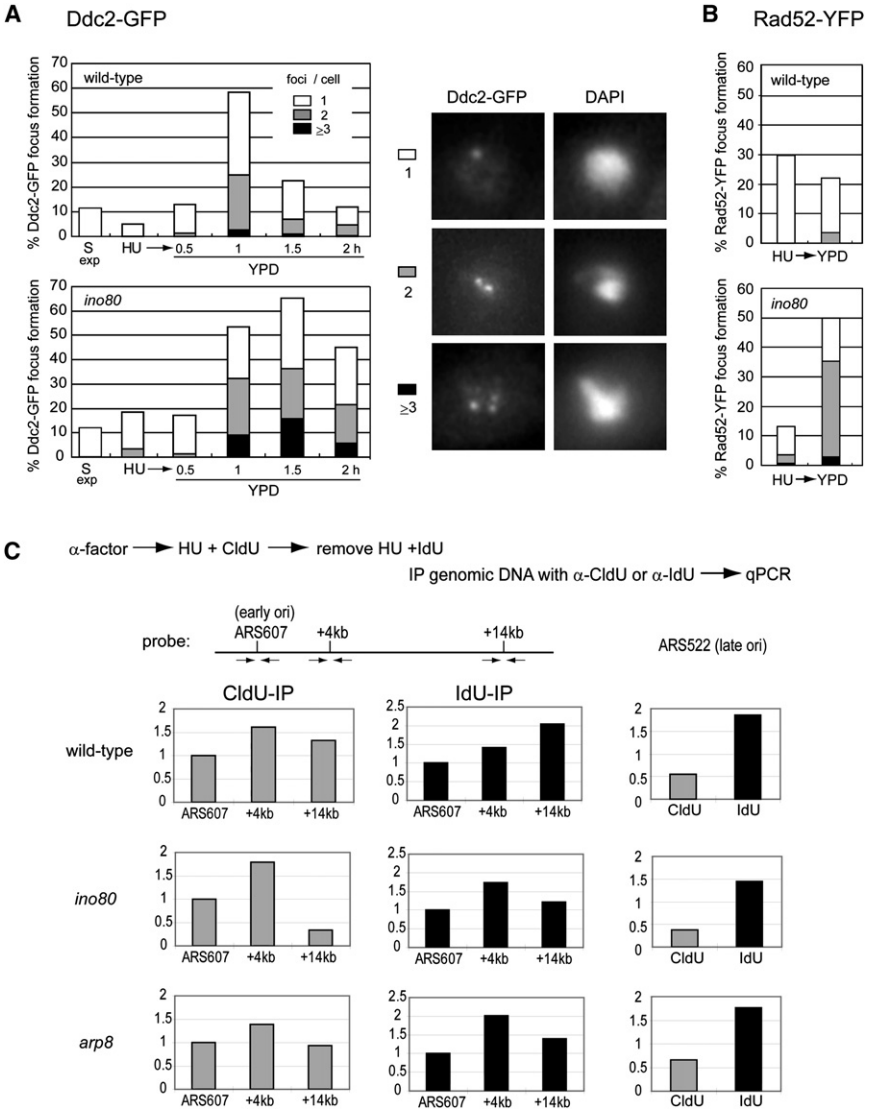

Figure 4. Recovery from Stalled Replication Forks Fails in *ino80* Mutants

(A) Isogenic wild-type and *ino80* cells bearing Ddc2-GFP were synchronized in G1 and blocked in 0.2 M HU for 90 min and then released into fresh YPD for the indicated times. The frequency of cells having one, two, or greater than three Ddc2-foci are plotted. Images of typical signals are shown. The level of Ddc2-GFP foci in S-phase cells of an exponential culture are labeled "S-exp." Over 100 cells are scored for each point.

(B) Isogenic wild-type (GA-4956) and *ino80* cells (GA-2264) expressing Rad52-YFP (pWJ1213, a gift form R. Rothstein) were cultured in SC-His. Cells were synchronously released into SC-His + 0.2M HU for 90 min and then were released into fresh SC-His for 2 hr. α-factor was added to the culture after 90 min to block the entry into next S phase. Frequency of cells having one, two, or greater than three Rad52-foci is plotted.

(C) Isogenic wild-type, *ino80*, and *arp8* cells bearing hENT1 and 8× TK were released synchronously into 0.2 M HU containing CldU for 1.5 hr. Cells were washed and released in fresh YPD containing IdU. After 45 min, cells were blocked prior to mitosis by nocodazole (15 μg/ml) and cultured for another 45 min. Genomic DNA was sonicated and denatured, and CldU and IdU incorporated DNA fragments were recovered by immunoprecipitation (see the Experimental Procedures for details). The distribution of label around origins was probed by real-time PCR for ARS607, ARS607+4k, ARS607+14k, and ARS522. The ratio of recovered IP/input DNA is normalized to that of ARS607.

arcs," which indicate initiation of DNA replication. By 2D gel analysis, the intensity of the bubble-arc signal was similar in the mutant and wild-type cells, arguing that initiation, per se, is not impaired. However, upon release from HU, the bubble arc in wild-type cells disappeared by 40 min as the replication fork moved along the DNA fiber (note the Y arc signal at +8 kb by 60 min; Figure 3C). In contrast, in *ino80* and *arp8* mutants, the replication bubbles persisted at the origin until 60 min and the Y arc signal at +8 kb remained strong. Although we did not detect fork collapse by 2D gel analysis in the form of a "cone" signal [30], *ino80* mutants, nonetheless, had significantly delayed or impaired resumption of DNA synthesis. Again, in the absence of HU, we detected only minor differences in origin firing between wild-type and mutant cells (Figure S5B).

Ddc2 Foci Accumulate, Generating Rad52 Foci as *ino80* Cells Recover from HU Arrest

Impaired fork recovery often leads to the formation of a repair focus enriched for Mec1-Ddc2, the budding yeast equivalent of ATR-ATRIP [15]. Mec1-Ddc2 accumulates at resected DSBs in a manner dependent on the single-strand binding factor RPA [31–33]. If stalled forks generate breaks that must be repaired by homologous recombination, then a focus of Rad52 forms. Because the severity of an S-phase insult can be quantified by scoring the frequency of either Ddc2 or Rad52 foci [34, 35], we examined whether loss of Ino80 activity enhances either the accumulation of foci containing either Ddc2-GFP or Rad52-YFP during the recovery from HU block.

Upon arrest in HU, wild-type cells had a single bright Ddc2 focus in only 5% of the cells. As cells were released from HU into rich medium, cells with a single Ddc2 focus transiently peaked at about 30% at 1 hr after release, and by 2 hr the value dropped again to 7%, indicating that <10% of wild-type cells had a persistent DSB or stalled fork (Figure 4A). In contrast nearly 20% of the *ino80* mutant cells had one or two bright Ddc2 foci upon HU arrest, and >30% of the mutant cells retained more than one persistent Ddc2 focus per cell 1 hr after removal of HU (Figure 4A). Finally, 15% of *ino80* cells had ≥3 Ddc2 foci by 1.5 hr after release, whereas multiple foci occurred in just 1% of wild-type cells.

Importantly, Ddc2-GFP foci were seen to persist >2 hr only in the mutant cells. This would argue that recovery is impossible or delayed, consistent with the loss of viability scored for the HU-treated *ino80* mutant (Figure 3A). We therefore scored for Rad52 foci to see if *ino80* cells were accumulating DSBs or simply single-strand DNA that would bind Mec1-Ddc2. We found that *ino80* cells actually form fewer Rad52 foci than wild-type cells when they were arrested in HU, but when the cells tried to recover from fork arrest, the number of

Rad52-YFP foci in the mutant increased, until >35% of the cells had more than one focus (Figure 4B). By contrast, the number of foci in wild-type cells decreased during recovery, indicating successful completion of repair. These differences in foci formation are not seen in randomly growing cultures: The rates of spontaneous Ddc2- and Rad52-focus formation in an unchallenged S phase are very similar in wild-type and in *ino80* mutant cells (Figure S6). This is consistent with the FACS data, which argue that the absence of Ino80 does not impair normal S phase progression (Figure S5). Rather, INO80 function is necessary to prevent fork collapse and the accumulation of unproductive recombination structures under conditions of fork stalling.

To monitor the efficiency with which these cells resume DNA synthesis, we used yeast cells carrying the herpes virus thymidine kinase (TK) and hENT1 genes to reconstitute a thymidine nucleotide salvage pathway [36]. These modified yeast cells efficiently incorporate derivatized thymidine analogs supplied in the culture media, such as IdU and CldU, allowing us to monitor newly synthesized DNA. The wild-type, *ino80*, and *arp8* cells carrying TK and hENT1 were synchronized in G1 and then allowed to grow for 90 min in media containing 0.2 M HU and CldU. A sample was taken and the remaining cells were released into fresh YPD containing IdU to monitor resumption of DNA synthesis. DNA fragments that had incorporated CldU or IdU were recovered by immunoprecipitation [16], and the enrichment of newly synthesized DNA at ARS607 or at the late origin ARS522 was quantified by qPCR (Figure 4C).

Wild-type cells efficiently incorporated CldU close to the early-firing origin ARS607 (Figure 4C). Moreover, after release from HU, the resumption of replication led to IdU incorporation in more distal origin fragments (+14 kb; Figure 4C). In *ino80* cells, consistent with our 2D gel analysis, we saw efficient incorporation of CldU at ARS607 as origins fired and the cells arrested in HU. Its incorporation was reduced at +14 kb, which indicates that fork progression was impaired on HU. More importantly, IdU incorporation did not increase at +14 kb during recovery from HU arrest, arguing that DNA synthesis failed to resume in the *ino80* mutant (Figure 4C). The low level of CldU and IdU incorporation at the late origin ARS522 on HU (half of ARS607 levels) confirmed that origin firing was blocked in both strains, although the ARS replicated efficiently after recovery from HU (see IdU signal; Figure 4C). This reinforces our interpretation that loss of Ino80 does not impair initiation or DNA synthesis in general but, specifically, the resumption of replication following fork arrest.

Rad53 Kinase Phosphorylation Persists in *ino80* Cells

The repression of late-firing origins on HU required activation of the downstream checkpoint kinase Rad53 [27]. To examine the efficiency of Rad53 activation in cells lacking the INO80 complex, we monitored Rad53 mobility in an SDS gel after exposure to HU because this shift is a sensitive measure of autophosphorylation and kinase activation. Indeed, in *ino80* and *arp5* cells exposed to 0.2 M HU, we see a robust shift in Rad53 to a more slowly migrating form after 60 and 90 min on HU (Figure 5). On MMS we even scored Rad53 hyperactivation in the *ino80* mutant (data not shown), although in response to a HO-induced DSB there is a delayed activation of Rad53 in *ino80* mutants [8]. This delayed checkpoint activation could reflect a role of INO80-mediated remodeling in efficient end-resection at the DSB.

We then assayed for the dephosphorylation and downregulation of Rad53 during the recovery phase after HU arrest. We find that the phosphorylated form of Rad53 persisted longer in the *ino80* and *arp5* mutants than in wild-type cells after release from the HU-induced arrest (Figure 5). This is consistent with the observed accumulation of Ddc2 and Rad52 foci and the delayed resumption of DNA synthesis after HU treatment. We conclude that the impaired recovery from replication fork stalling that occurs in Ino80-deficient cells leads to a prolonged damage response.

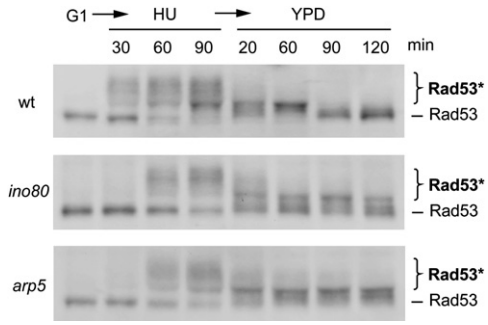

Figure 5. Downregulation of Rad53 Phosphorylation Is Delayed during the Recovery from Fork Arrest in *ino80* Cells

Exponentially growing wild-type (GA-4956), *ino80* (GA-2264), and *arp5* (GA-2181) mutant cells were synchronized with α-factor in G1 and released into YPAD + 0.2 M HU. After 90 min cells were washed and released into fresh YPD for the indicated times. Rad53 mobility shift (Rad53*) was monitored at the indicated time points. Rad53 was detected with anti-Rad53 antibody (yC-19, Santa Cruz).

Discussion

Here, we show that the INO80 chromatin-remodeling complex is associated with stalled replication forks genome wide. Consistently, strains lacking Ino80 show significant defects in the resumption of DNA replication, as monitored by an inability to resume DNA replication, an accumulation of Rad52-bound repair foci, and the ensuing hyperactivation and persistence of the checkpoint response. Although we do not formally exclude the possibility that some of the phenotypes are compounded by a misregulation of gene expression in *ino80* mutants, the striking accumulation of the INO80 complex at stalled forks near origins and at replication-fork barriers such as the rDNA RFB and tRNA genes argues that it is likely to act directly in DNA fork recovery.

We have shown a highly significant loss in recovery from HU-induced fork stalling in cells lacking Ino80. This is manifest as a reduction in the ability to incorporate derivatized NTP by DNA replication after HU removal, the accumulation and persistence of Mec1-Ddc2 and Rad52 foci, and increased cell death (Figures 2–4). Because Ino80 is present at stalled forks, we propose that the INO80 complex directly promotes DNA polymerase resumption in the vicinity of the fork by modulating chromatin status through its ability to either remodel or remove histone octamers [5, 8, 37]. The fact that we observe similar phenotypes with *arp5* or *arp8* mutations is a compelling argument that the enzymatic activity of the complex is required for fork resumption. Loss of these subunits was shown to impair histone remodeling without disrupting the complex entirely [17].

It is intriguing that we also detect Ino80 at unfired origins in G1 phase cells and at late-firing origins when cultures are arrested in HU. We note that two subunits of the INO80 complex, Arp4 and Rvb2, were recovered in a fraction containing

purified ORC (C.A. Fox, personal communication). It is unlikely, however, that Arp4 or Rvb1/2 alone can account for the recruitment of INO80 to origins. The SWR1 complex also contains the Arp4 and Rvb1/2 subunits, and in a separate study we have monitored the chromosomal distribution of Swr1 and Arp6 in a series of ChIP-chip experiments. Importantly, <20% of the ARS elements bind the SWR1 complex in a randomly growing culture, and in the presence of HU the percentage actually drops to 5%, which is opposite of the INO80 response (T. Yoshida and M. H., unpublished data). Consistently, the *swr1* null allele does not show sensitivity to HU [4]. Loss of the variant histone H2A.Z, which the SWR1 complex deposits, also did not influence survival on HU or fork movement [38]. Thus, although Rvb1/2 may contribute to basal levels of interaction, HU-induced recruitment appears to be specific for INO80.

It is important to note that the binding of the INO80 complex at promoters and tRNA genes did not change in cells arrested in high HU (Figure S4). Thus, the enhanced binding of INO80 at stalled forks and at repressed origins is specific. Its specificity may be enhanced by activation of the checkpoint response. The binding of Ino80 at late-firing origins could reflect association of the complex with components of ORC, the pre-replication complex, or another DNA-bound factor. The INO80 Ies4 subunit already has been reported to be a target of Mec1-Ddc2 kinase [39], and this and/or a similar modification may be responsible for the increased binding seen on HU. Alternatively, checkpoint-induced modifications might enhance the affinity of the complex for aberrant DNA structures such as those accumulated at stalled replication forks. This mechanism has been proposed for the recruitment of human INO80 by YY1 [10]. In any case, the fact that Ino80 enrichment on HU is site specific makes it clear that multiple pathways lead to INO80 recruitment and that only some of these are sensitive to checkpoint activation. Further analysis is needed to identify which of the 13 subunits of the INO80 complex mediate its affinity for different sites.

From FACS and 2D gel analyses, we argue that the INO80 complex is not required for origin firing per se but, rather, for resumption of replication by stalled polymerases. The observed lack of fork recovery may lead to an enhanced dependence on recombinational repair ,which was observed to be compromised both in *ino80* mutants in yeast [9] and when YY1 or Ino80 was depleted in human cells [10]. We note that synthetic growth defects were reported between mutants in *arp8* and mutations in either *rad55* or *rad59*, which are implicated in recombinational repair [40]. Furthermore, genome-wide synthetic lethal screening also suggests that Arp8 interacts genetically with Rad27 (a protein implicated both in repair and in Okazaki fragment processing), Ctf4 (pol α associated protein), and Pol32 (the third subunit of pol δ) [41, 42]. Pol32 is required for translesion synthesis when replication forks encounter damage [43] and break-induced replication [44].

These genetic results suggest that alternative fork-related repair mechanisms become critical when the INO80 complex is not functional at stalled forks. It is not yet clear whether Ino80 promotes one particular mode of fork recovery or, alternatively, removes histones and other impediments to facilitate various pathways of fork resumption (reviewed in [15]). Arp8 or Ino80 function becomes necessary for survival in cells in which re-replication of DNA is forced by a manipulation of ORC and Cdc6 [45] (bioPIXIE [23]) and in cells that depend on nonreciprocal recombination-mediated events between telomeres, such as break-induced repair, for telomere maintenance [46]. These defects could all reflect INO80's role in promoting stalled replication-fork recovery.

How does the recruitment and function of INO80 at stalled forks differ from its role at DSBs? At DSBs the INO80 complex recognizes and helps evict a phosphorylated form of H2A (called γH2AX in mammals) [6–8, 40], largely through its small subunit Nhp10 [40]. Although H2A becomes phosphorylated in a Mec1-dependent manner at stalled replication forks [28], we found that the recruitment of Arp5 to ARS607 on HU occurs independently of γH2A (see Arp5 ChIP in the *hta1/2* S129* mutant; Figure S7). Consistently, deletion of *nhp10* failed to provoke the same loss of viability as *ino80* or *arp5* mutants during recovery from HU arrest (data not shown). Thus, unlike the situation at a DSB, we speculate that yeast may have a "recombination structure" recognizing factor similar to YY1 [10], which could be crucial for recruiting the INO80 complex to unusual structures at stalled forks, preventing their breakage during crucial steps in the resumption of replication fork progression.

Experimental Procedures

Yeast Techniques

All yeast strains are listed in Table S1. Cell culture used standard YPD or SC media at 30°C. Pheromone synchronization, HU arrest, and release were performed as described [28, 47]. For G2/M arrest, cells were cultured in 15 μg/ml nocodazole YPD 1% DMSO for 3 hr. FACS analysis was performed as described in [48]; see also the Supplemental Experimental Procedures. Two-dimensional gel analysis was carried out essentially as described in [48], except that cells were spheroplasted with 100 U/ml lyticase in QIAGEN Y1 buffer for 30 min at 30°C, and genomic DNA was isolated with QIAGEN G20 tips. Replication intermediates were detected with DIG-labeled probes as indicated (Roche, DIG Application Manual).

ChIP-Chip Assays

ChIPs with the appropriate Dynabeads (DYNAL) were performed as previously described [16] with either anti-Myc monoclonal antibody (9E11; Abcam, ab56) or an anti-Arp5 polyclonal antibody. Further details are provided in the Supplemental material. Microarrays were scanned by GeneChip Scanner 3000 7G (Affymetrix), and data analysis was performed as previously described [49].

ChIP and qPCR

Ino80-Avi ChIP was performed essentially as described in [24] with an Ino80- myc-Avi tag and an isogenic nontagged strain transformed with pRS415-NLS-BirA. Growth media was supplemented with 20 nM biotin. For TK normalization, 1×10^7 cells of GA-4563 (8× TK) were added to the culture prior to fixation with 1% formaldehyde for 30 min at 25°C. Cell lysis, immunoprecipitation, and crosslink reversal were done as described in [24] except that streptavidin-Dynal bead incubation with cell extracts was carried out at 4°C for 3 hr. Input and immunoprecipitated DNA was purified as described in [48]. Ino80-13myc and Pol2-13myc ChIP was carried out as described in [48] with anti-Myc 9E10 antibody, and precipitated DNA was quantified with real-time PCR by using Taqman probes or SYBR green. For the incorporation and ChIP on CldU and IdU incorporation, see the Supplemental Data. The Ct values of a seeded TK gene or else of the endogenous locus *FAB1* were used for background determination. Sequence information of probes and primers is available upon request.

Microscopy

Wild-type and *ino80* cells bearing one genomic copy of *DDC2-GFP* or the plasmid-borne *RAD52-YFP* (pWJ1213) were synchronously released from a G1 block into 0.2 M HU for 90 min. Cells were washed and released into fresh medium then analyzed by the microscopy at indicated times or at 2 hr for Rad52-YFP. A Metamorph-driven Olympus IX70 microscope was used to capture 21 image stacks of 0.2 μm step size. More than 100 cells are scored for each time point.

Accession Numbers

ChIP-chip data are available at the GEO database under accession number GSE9421.

Supplemental Data

Additional Experimental Procedures, seven figures, and one table are available at http://www.current-biology.com/cgi/content/full/18/8/566/DC1/.

Acknowledgments

We thank H.L. Klein, X. Shen, and L. Bjergbaek for yeast strains; O.M. Aparicio for hENT1-TK plasmid; R. Rothstein for Rad52-YFP plasmid (pWJ1213), and T. Yoshida and C.A. Fox for communication of unpublished results. We are grateful to I. Takehiko and K. Shirahige for the technical advice, L. Gehlen for statistical analysis, and D. Schübeler, M. Schwaiger, and V. Dion for critically reading the manuscript. The research was funded by a basic research grant from the Bio-oriented Technology Research Advancement Institution (to K.O.), Grant-in-Aids for Scientific Research of Priority Areas from the Ministry of Education, Culture, Sports, Science, and Technology, Japan (to K.O. and M.H.), the Swiss NCCR Frontiers-in-Genetics, and the Novartis Research Foundation.

Received: January 28, 2008
Revised: March 16, 2008
Accepted: March 26, 2008
Published online: April 10, 2008

References

1. Lusser, A., and Kadonaga, J.T. (2003). Chromatin remodeling by ATP-dependent molecular machines. Bioessays *25*, 1192–1200.
2. Krogan, N.J., Keogh, M.C., Datta, N., Sawa, C., Ryan, O.W., Ding, H., Haw, R.A., Pootoolal, J., Tong, A., Canadien, V., et al. (2003). A Snf2 family ATPase complex required for recruitment of the histone H2A variant Htz1. Mol. Cell *12*, 1565–1576.
3. Kobor, M.S., Venkatasubrahmanyam, S., Meneghini, M.D., Gin, J.W., Jennings, J.L., Link, A.J., Madhani, H.D., and Rine, J. (2004). A protein complex containing the conserved Swi2/Snf2-related ATPase Swr1p deposits histone variant H2A.Z into euchromatin. PLoS Biol. *2*, e131. 10.1371/journal.pbio.0020131.
4. Mizuguchi, G., Shen, X., Landry, J., Wu, W.H., Sen, S., and Wu, C. (2004). ATP-driven exchange of histone H2AZ variant catalyzed by SWR1 chromatin remodeling complex. Science *303*, 343–348.
5. Shen, X., Mizuguchi, G., Hamiche, A., and Wu, C. (2000). A chromatin remodelling complex involved in transcription and DNA processing. Nature *406*, 541–544.
6. van Attikum, H., Fritsch, O., Hohn, B., and Gasser, S.M. (2004). Recruitment of the INO80 complex by H2A phosphorylation links ATP-dependent chromatin remodeling with DNA double-strand break repair. Cell *119*, 777–788.
7. Tsukuda, T., Fleming, A.B., Nickoloff, J.A., and Osley, M.A. (2005). Chromatin remodelling at a DNA double-strand break site in Saccharomyces cerevisiae. Nature *438*, 379–383.
8. van Attikum, H., Fritsch, O., and Gasser, S.M. (2007). Distinct roles for SWR1 and INO80 chromatin remodeling complexes at chromosomal double-strand breaks. EMBO J. *26*, 4113–4125.
9. Kawashima, S., Ogiwara, H., Tada, S., Harata, M., Wintersberger, U., Enomoto, T., and Seki, M. (2007). The INO80 complex is required for damage-induced recombination. Biochem. Biophys. Res. Commun. *355*, 835–841.
10. Wu, S., Shi, Y., Mulligan, P., Gay, F., Landry, J., Liu, H., Lu, J., Qi, H.H., Wang, W., Nickoloff, J.A., et al. (2007). A YY1–INO80 complex regulates genomic stability through homologous recombination-based repair. Nat. Struct. Mol. Biol. *14*, 1165–1172.
11. Jonsson, Z.O., Jha, S., Wohlschlegel, J.A., and Dutta, A. (2004). Rvb1p/Rvb2p recruit Arp5p and assemble a functional Ino80 chromatin remodeling complex. Mol. Cell *16*, 465–477.
12. Jin, J., Cai, Y., Yao, T., Gottschalk, A.J., Florens, L., Swanson, S.K., Gutierrez, J.L., Coleman, M.K., Workman, J.L., Mushegian, A., et al. (2005). A mammalian chromatin remodeling complex with similarities to the yeast INO80 complex. J. Biol. Chem. *280*, 41207–41212.
13. Squatrito, M., Gorrini, C., and Amati, B. (2006). Tip60 in DNA damage response and growth control: Many tricks in one HAT. Trends Cell Biol. *16*, 433–442.
14. Bao, Y., and Shen, X. (2007). Chromatin remodeling in DNA double-strand break repair. Curr. Opin. Genet. Dev. *17*, 126–131.
15. Tourriere, H., and Pasero, P. (2007). Maintenance of fork integrity at damaged DNA and natural pause sites. DNA Repair (Amst.) *6*, 900–913.
16. Katou, Y., Kanoh, Y., Bando, M., Noguchi, H., Tanaka, H., Ashikari, T., Sugimoto, K., and Shirahige, K. (2003). S-phase checkpoint proteins Tof1 and Mrc1 form a stable replication-pausing complex. Nature *424*, 1078–1083.
17. Shen, X., Ranallo, R., Choi, E., and Wu, C. (2003). Involvement of actin-related proteins in ATP-dependent chromatin remodeling. Mol. Cell *12*, 147–155.
18. Sharp, P.M., and Lloyd, A.T. (1993). Regional base composition variation along yeast chromosome III: Evolution of chromosome primary structure. Nucleic Acids Res. *21*, 179–183.
19. Bradnam, K.R., Seoighe, C., Sharp, P.M., and Wolfe, K.H. (1999). G+C content variation along and among Saccharomyces cerevisiae chromosomes. Mol. Biol. Evol. *16*, 666–675.
20. Dujon, B. (1996). The yeast genome project: What did we learn? Trends Genet. *12*, 263–270.
21. Ivessa, A.S., Lenzmeier, B.A., Bessler, J.B., Goudsouzian, L.K., Schnakenberg, S.L., and Zakian, V.A. (2003). The Saccharomyces cerevisiae helicase Rrm3p facilitates replication past nonhistone protein-DNA complexes. Mol. Cell *12*, 1525–1536.
22. Azvolinsky, A., Dunaway, S., Torres, J.Z., Bessler, J.B., and Zakian, V.A. (2006). The S. cerevisiae Rrm3p DNA helicase moves with the replication fork and affects replication of all yeast chromosomes. Genes Dev. *20*, 3104–3116.
23. Myers, C.L., Robson, D., Wible, A., Hibbs, M.A., Chiriac, C., Theesfeld, C.L., Dolinski, K., and Troyanskaya, O.G. (2005). Discovery of biological networks from diverse functional genomic data. Genome Biol. *6*, R114. 10.1186/gb-2005-6-13-r114.
24. van Werven, F.J., and Timmers, H.T. (2006). The use of biotin tagging in Saccharomyces cerevisiae improves the sensitivity of chromatin immunoprecipitation. Nucleic Acids Res. *34*, e33. 10.1093/nar/gkl003.
25. Brewer, B.J., Lockshon, D., and Fangman, W.L. (1992). The arrest of replication forks in the rDNA of yeast occurs independently of transcription. Cell *71*, 267–276.
26. Kobayashi, T. (2003). The replication fork barrier site forms a unique structure with Fob1p and inhibits the replication fork. Mol. Cell. Biol. *23*, 9178–9188.
27. Santocanale, C., and Diffley, J.F. (1998). A Mec1- and Rad53-dependent checkpoint controls late-firing origins of DNA replication. Nature *395*, 615–618.
28. Cobb, J.A., Schleker, T., Rojas, V., Bjergbaek, L., Tercero, J.A., and Gasser, S.M. (2005). Replisome instability, fork collapse, and gross chromosomal rearrangements arise synergistically from Mec1 kinase and RecQ helicase mutations. Genes Dev. *19*, 3055–3069.
29. Paciotti, V., Clerici, M., Scotti, M., Lucchini, G., and Longhese, M.P. (2001). Characterization of mec1 kinase-deficient mutants and of new hypomorphic mec1 alleles impairing subsets of the DNA damage response pathway. Mol. Cell. Biol. *21*, 3913–3925.
30. Lopes, M., Cotta-Ramusino, C., Pellicioli, A., Liberi, G., Plevani, P., Muzi-Falconi, M., Newlon, C.S., and Foiani, M. (2001). The DNA replication checkpoint response stabilizes stalled replication forks. Nature *412*, 557–561.
31. Zou, L., and Elledge, S.J. (2003). Sensing DNA damage through ATRIP recognition of RPA-ssDNA complexes. Science *300*, 1542–1548.
32. Dubrana, K., van Attikum, H., Hediger, F., and Gasser, S.M. (2007). The processing of double-strand breaks and binding of single-strand-binding proteins RPA and Rad51 modulate the formation of ATR-kinase foci in yeast. J. Cell Sci. *120*, 4209–4220.
33. Rouse, J., and Jackson, S.P. (2002). Lcd1p recruits Mec1p to DNA lesions in vitro and in vivo. Mol. Cell *9*, 857–869.
34. Lisby, M., Barlow, J.H., Burgess, R.C., and Rothstein, R. (2004). Choreography of the DNA damage response: Spatiotemporal relationships among checkpoint and repair proteins. Cell *118*, 699–713.
35. Meister, P., Taddei, A., Vernis, L., Poidevin, M., Gasser, S.M., and Baldacci, G. (2005). Temporal separation of replication and recombination requires the intra-S checkpoint. J. Cell Biol. *168*, 537–544.

36. Viggiani, C.J., and Aparicio, O.M. (2006). New vectors for simplified construction of BrdU-Incorporating strains of Saccharomyces cerevisiae. Yeast *23*, 1045–1051.
37. Tsukiyama, T. (2002). The in vivo functions of ATP-dependent chromatin-remodelling factors. Nat. Rev. Mol. Cell Biol. *3*, 422–429.
38. Dhillon, N., Oki, M., Szyjka, S.J., Aparicio, O.M., and Kamakaka, R.T. (2006). H2A.Z functions to regulate progression through the cell cycle. Mol. Cell. Biol. *26*, 489–501.
39. Morrison, A.J., Kim, J.A., Person, M.D., Highland, J., Xiao, J., Wehr, T.S., Hensley, S., Bao, Y., Shen, J., Collins, S.R., et al. (2007). Mec1/Tel1 phosphorylation of the INO80 chromatin remodeling complex influences DNA damage checkpoint responses. Cell *130*, 499–511.
40. Morrison, A.J., Highland, J., Krogan, N.J., Arbel-Eden, A., Greenblatt, J.F., Haber, J.E., and Shen, X. (2004). INO80 and gamma-H2AX interaction links ATP-dependent chromatin remodeling to DNA damage repair. Cell *119*, 767–775.
41. Collins, S.R., Miller, K.M., Maas, N.L., Roguev, A., Fillingham, J., Chu, C.S., Schuldiner, M., Gebbia, M., Recht, J., Shales, M., et al. (2007). Functional dissection of protein complexes involved in yeast chromosome biology using a genetic interaction map. Nature *446*, 806–810.
42. Pan, X., Ye, P., Yuan, D.S., Wang, X., Bader, J.S., and Boeke, J.D. (2006). A DNA integrity network in the yeast Saccharomyces cerevisiae. Cell *124*, 1069–1081.
43. Hanna, M., Ball, L.G., Tong, A.H., Boone, C., and Xiao, W. (2007). Pol32 is required for Pol zeta-dependent translesion synthesis and prevents double-strand breaks at the replication fork. Mutat. Res. *625*, 164–176.
44. Lydeard, J.R., Jain, S., Yamaguchi, M., and Haber, J.E. (2007). Break-induced replication and telomerase-independent telomere maintenance require Pol32. Nature *448*, 820–823.
45. Archambault, V., Ikui, A.E., Drapkin, B.J., and Cross, F.R. (2005). Disruption of mechanisms that prevent rereplication triggers a DNA damage response. Mol. Cell. Biol. *25*, 6707–6721.
46. Yu, E.Y., Steinberg-Neifach, O., Dandjinou, A.T., Kang, F., Morrison, A.J., Shen, X., and Lue, N.F. (2007). Regulation of telomere structure and functions by subunits of the INO80 chromatin remodeling complex. Mol. Cell. Biol. *27*, 5639–5649.
47. Cobb, J.A., Bjergbaek, L., Shimada, K., Frei, C., and Gasser, S.M. (2003). DNA polymerase stabilization at stalled replication forks requires Mec1 and the RecQ helicase Sgs1. EMBO J. *22*, 4325–4336.
48. Shimada, K., Pasero, P., and Gasser, S.M. (2002). ORC and the intra-S-phase checkpoint: A threshold regulates Rad53p activation in S phase. Genes Dev. *16*, 3236–3252.
49. Katou, Y., Kaneshiro, K., Aburatani, H., and Shirahige, K. (2006). Genomic approach for the understanding of dynamic aspect of chromosome behavior. Methods Enzymol. *409*, 389–410.
50. Nieduszynski, C.A., Hiraga, S., Ak, P., Benham, C.J., and Donaldson, A.D. (2007). OriDB: A DNA replication origin database. Nucleic Acids Res. *35*, D40–D46.